# Fabrication and characterization of controlled release poly(D,L-lactide-*co*-glycolide) millirods

**Feng Qian, Agata Szymanski, Jinming Gao**
*Cancer-Targeted Drug Delivery Laboratory, Department of Biomedical Engineering, Case Western Reserve University, 10900 Euclid Avenue, Cleveland, Ohio 44106*

Received 18 August 2000; accepted 5 October 2000

**Abstract:** A compression–heat molding procedure was developed to fabricate poly(D,L-lactide-*co*-glycolide) (PLGA) controlled release drug delivery devices for the local treatment of tumors. The drug delivery devices were designed in the shape of a cylindrical millirod (1.6-mm diameter, 10-mm length), which allows them to be implanted by a modified 14-gauge tissue biopsy needle into tumor tissues via image-guided interventional procedures. In this study, the prototype trypan blue-containing PLGA millirods were fabricated under a compression pressure of $4.6 \times 10^6$ Pa and different fabrication temperatures for 2 h. The scanning electron microscopy results showed complete polymer annealing for millirods fabricated at 80 and 90°C, while the cross sections of the 60 and 70°C millirods showed incompletely annealed PLGA microspheres and trypan blue powders. The density, flexural modulus, and release properties of the PLGA millirods were also characterized and compared. The average values of the density and flexural modulus of the millirods increased with an increase in fabrication temperature. The flexural modulus values of most PLGA millirods were above $1 \times 10^8$ Pa, which provides sufficient stiffness for implantation within the tumor tissue. In addition, a $\Delta c_p$ method was developed to determine the loading density of trypan blue in the PLGA millirods by differential scanning calorimetry. Results from the $\Delta c_p$ measurement showed that trypan blue was homogeneously distributed in the millirod. Release studies in phosphate-buffered saline showed that the release rate decreased for the millirods fabricated at higher temperatures. The times for the release of 50% trypan blue were 5, 25, 25, and 25 h for millirods fabricated at 60, 70, 80, and 90°C, respectively. Millirods fabricated at 90°C had the most reproducible release profiles. The results from this study established compression–heat molding as an effective method to fabricate controlled release PLGA millirods with sufficient mechanical strength and reproducible release profiles for local cancer therapy. © 2001 John Wiley & Sons, Inc. J Biomed Mater Res 55: 512–522, 2001

**Key words:** controlled release drug delivery; poly(D,L-lactide-*co*-glycolide); compression–heat molding; polymer characterization

## INTRODUCTION

Advances in imaging and interventional technology have profoundly impacted the medical treatment of cancer over the past decade. Image-guided thermal ablation of solid tumors is emerging as a novel technique for the minimally invasive treatment of tumors.[1–8] In this procedure a physician inserts a needle electrode under image guidance into a tumor percutaneously and with image feedback controls ablation by adjusting the duration and electrical current in the electrode. The alternating electric current causes local ionic agitation and frictional heat, which increases the tissue temperature to 70–90°C to kill the cancerous cells. This novel interventional procedure has been applied to treat various types of cancers, including squamous cell carcinoma of the head and neck,[9] primary brain tumors,[10] and cancers of the liver,[11–15] prostate,[16] pancreas,[17,18] kidney,[19–21] and breast.[22,23] Image-guided ablation permits accurate local destruction of solid tumors and only requires local anesthesia. Although patients currently stay overnight at the hospital after treatment, tumor ablation has the potential to become an outpatient procedure. However, tumor recurrence has been reported following various ablation treatments and limits the scope of their applications.[24–27] The long-term goal of this project is to develop a local drug therapy to prevent tumor recurrence. This therapy consist of a drug containing poly(D,L-lactide-*co*-glycolide) (PLGA) millirod, which is directly implanted into ablated tumors and delivers elevated concentrations of anticancer drugs to kill any viable tumor cells remaining after thermoablation.

Correspondence to: Dr. J. Gao; e-mail: jmg23@po.cwru.edu
Contract grant sponsor: Whitaker Foundation; Contract grant number: RG-99-0342

The objective of this study was to develop an effective procedure to fabricate PLGA millirods with reproducible release profiles. PLGA is a biocompatible and biodegradable polymer with a wide range of pharmaceutical applications. Various forms of controlled release devices, including tablets,[28] microspheres,[29–32] and nanoparticles,[33–36] are fabricated from PLGA. The Food and Drug Administration considers this polymer to be safe in drug delivery applications. The geometry of the current delivery device was designed in the shape of a cylindrical millirod (1.6-mm diameter, 1-cm length), which permits the direct implantation of the device into tumor tissue by a modified 14-gauge tissue biopsy needle under image-guided procedures.

We describe the compression–heat molding procedure used to fabricate the PLGA millirods that contain a dye molecule, trypan blue, and the means used to evaluate the reproducibility of this fabrication process. We used dynamic mechanical analysis (DMA), differential scanning calorimetry (DSC), and scanning electron microscopy (SEM) to characterize the mechanical properties, composition homogeneity, and microstructure and morphology of the millirods, respectively. The experimental results demonstrate that compression–heat molding is a successful procedure for the fabrication of PLGA millirods with reproducible release profiles and adequate mechanical strength for controlled release applications.

## MATERIALS AND METHODS

### Materials

PLGA (1:1 lactide:glycolide, 50,000 Da molecular weight, 0.65 dL/g inherent viscosity) was purchased from Birmingham Polymers, Inc. (Birmingham, AL). Trypan blue and poly(vinyl alcohol) (PVA, 13,000–23,000 Da molecular weight, 87–89% hydrolyzed) were purchased from Aldrich (Milwaukee, WI). Phosphate-buffered saline (PBS) and methylene chloride were obtained from Fisher Scientific (Pittsburgh, PA). Teflon tubes were purchased from McMaster–Carr Supply Company (Cleveland, OH).

### Preparation of PLGA microspheres and trypan blue powders

PLGA microspheres were produced using a single-emulsion procedure. The PLGA polymer was first dissolved in $CH_2Cl_2$ at 100 mg/mL, and 1 mL of this solution was added to 10 mL of aqueous PVA solution (1% w/w). The mixture was stirred vigorously by a homogenizer (model 985370, Biospec Products, Inc.) at 25,000–30,000 rpm for 1 min. The emulsion was then poured into a beaker containing 300 mL of the PVA solution. The bulk solution was stirred by a magnetic bar at 400 rpm overnight to allow the evaporation of the $CH_2Cl_2$. After solvent evaporation, the microspheres were collected by centrifugation, washed 3 times with distilled water, and freeze-dried by a lyophilizer. The PLGA microspheres were sieved by a 100-mesh sieve before the millirod fabrication. SEM was used to determine the size of the microspheres by measuring the diameter of 50 microspheres in an SEM picture and then taking an average value. The size of the PLGA microspheres was also measured by a BI-240 laser scattering particle sizer (Brookhaven Instruments).

The trypan blue from commercial sources was in the form of large 2–3-mm pieces. To convert these pieces into fine powders, the trypan blue was first dissolved in distilled water at a concentration of 50 mg/mL, and then the solution was lyophilized overnight. After freeze-drying the materials were loose and porous and were easily ground to fine powder with a mortar and pestle. The morphology of the trypan blue particles was examined by SEM.

### Fabrication of PLGA millirods by compression–heat molding

Figure 1 illustrates the experimental setup for the fabrication of PLGA millirods. The trypan blue powder and PLGA microspheres were first weighed separately according to the final loading density (20 w/w%) of trypan blue in the millirod. The two components were placed in a plastic tube and physically mixed by a vortex for 10 min. For each millirod 50 mg of the mixture was weighed and placed into a Teflon tube (1.6-mm i.d., 2.0-mm o.d.). Then the Teflon tube was placed inside a stainless steel mold, and a stainless steel plunger (1.6-mm diameter, 35-mm length) was inserted into each end of the Teflon tube. Before insertion of the Teflon

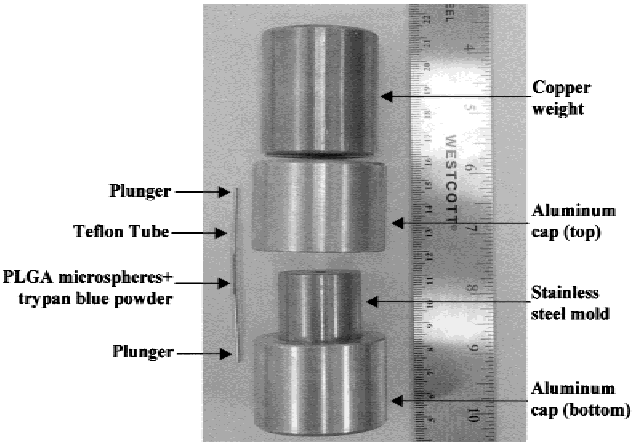


**Figure 1.** An illustration of the experimental setup for the fabrication of PLGA millirods by compression–heat molding. During fabrication, the Teflon tube containing the sample was placed inside a stainless steel mold and a constant compression pressure was applied by the gravity of a copper weight and aluminum cap. The setup was designed by the authors and produced by the machine shop at Case Western Reserve University.

tube, the mold, plungers, and other fabrication equipment were equilibrated to the oven temperature overnight. Two aluminum cap holders were placed on both sides of the stainless steel mold (Fig. 1). A copper weight (820 g) was placed on top of the aluminum cap to introduce a constant compression force to the mixture of PLGA microspheres and trypan blue powder. The whole system was placed into an iso-temp oven (set point accuracy <2°C, model 282A, Fisher) for 2 h to allow the annealing of the PLGA polymer. After polymer annealing, the PLGA millirod was cooled to room temperature and removed from the Teflon tube. The fabrication temperature was controlled at 60, 70, 80, and 90°C; eight millirods were fabricated for each temperature.

To determine the density of the millirod, the weight, length, and diameter of each millirod were measured. The diameter was measured as an average value from three different positions along the millirod axis, and it was used to calculate the volume of the millirod. The density was calculated by dividing the mass of the millirod by its volume.

### SEM analysis

A scanning electron microscope (model 840, JEOL) was used to study the surface morphology of the PLGA microspheres, trypan blue powder, and PLGA millirods. The outer surface and the cross section of the millirods were examined. The cross section was obtained by first creating a small crack at the millirod surface with a razor blade and then manually fracturing the millirod by force. Before SEM analysis the samples were mounted on the aluminum stubs by double-sided tape and sputter coated with Pd (10-nm thickness). The SEM analysis was carried out at an accelerating voltage of 20 kV.

### Mechanical analysis of PLGA millirods

The flexural modulus of each PLGA millirod was measured by a PerkinElmer DMA-7e dynamic mechanical analyzer. The DMA instrument worked in 3-point bending mode. The compression probe was tared before each measurement. The distance between the two parallel sample stages was 5 mm. The PLGA millirod was placed in the middle of the stages and perpendicular to the edge of each stage. The compression probe was lowered until it touched the surface of the millirod. A force of 100 mN was applied from the probe to the PLGA millirod, and the position of the probe at this position was read as zero. The DMA was then programmed to work in static stress scan mode; the initial and maximal forces were set at 100 and 2000 mN, respectively. The force scan rate was 200 mN/min. After the measurement, the modulus–strain curve was calculated with Pyris software. The flexural modulus at a higher strain value appeared to be a constant and was used to compare the millirods under different fabrication conditions.

### DSC analysis and measurement of loading density

The glass-transition temperature ($T_g$) and change in specific heat capacity ($\Delta c_p$) between the glassy and rubbery states of the PLGA polymer were measured by a Perkin–Elmer DSC-7 calorimeter. For all the experiments, samples of 5–10 mg were accurately weighed by a Perkin Elmer AD-4 autobalance and sealed into an aluminum sample pan. An empty aluminum pan was used as the reference sample. The DSC heating and cooling rates were controlled at 15°C/min, and all the experiments were carried out under a nitrogen purge (30 psi). Each sample was heated and cooled for five cycles between 10 and 80°C. The heating–cooling cycles permitted the elimination of any previous thermal history of the polymer and allowed the measurement of the polymer properties under reproducible conditions. The $\Delta c_p$ and $T_g$ values were measured by the Pyris software based on the last three heating thermograms.

To determine the composition homogeneity of trypan blue in the PLGA millirods, each of three millirods containing trypan blue was cut into five sections and the $\Delta c_p$ of each section was measured. The dye loading density in each section of the millirod was calculated from the $\Delta c_p$ values of this section and pure PLGA polymer based on Equation (4).

### *In vitro* release study

The release study was carried out in PBS (pH 7.4) at 37°C. Each millirod containing the trypan blue (10-mm length) was placed in a plastic vial containing 10 mL of PBS buffer. The sample vials were placed in an orbital shaker (model C24, New Brunswick Scientific) with a rotating speed of 100 rpm. At each time point the millirod was removed with forceps and placed into another vial with fresh PBS solution. The concentration of released trypan blue in the PBS buffer was determined at its maximum adsorption wavelength of 597.2 nm by a Hitachi U3210 UV–vis spectrophotometer. The extinction coefficient of trypan blue at this wavelength was measured to be 64.6 mL/(cm mg). The percentage of cumulative release was obtained by normalizing the released dye to the total amount of entrapped trypan blue in the PLGA millirods. The release study was carried out for 3 weeks until over 90% of the dye was released.

## RESULTS AND DISCUSSION

### Morphology of PLGA microspheres and trypan blue powder

In this study we used a physical mixture of PLGA microspheres and trypan blue powder to fabricate the drug delivery device. The morphology, size, and size distribution of the PLGA microspheres and trypan blue powder can affect the release profiles of trypan blue from the PLGA matrix. We used SEM to characterize the morphological properties of these particles. Figure 2(a) shows the SEM image of PLGA microspheres fabricated from a single emulsion procedure. In this procedure the average size of the PLGA microspheres can be controlled by the concentration of the

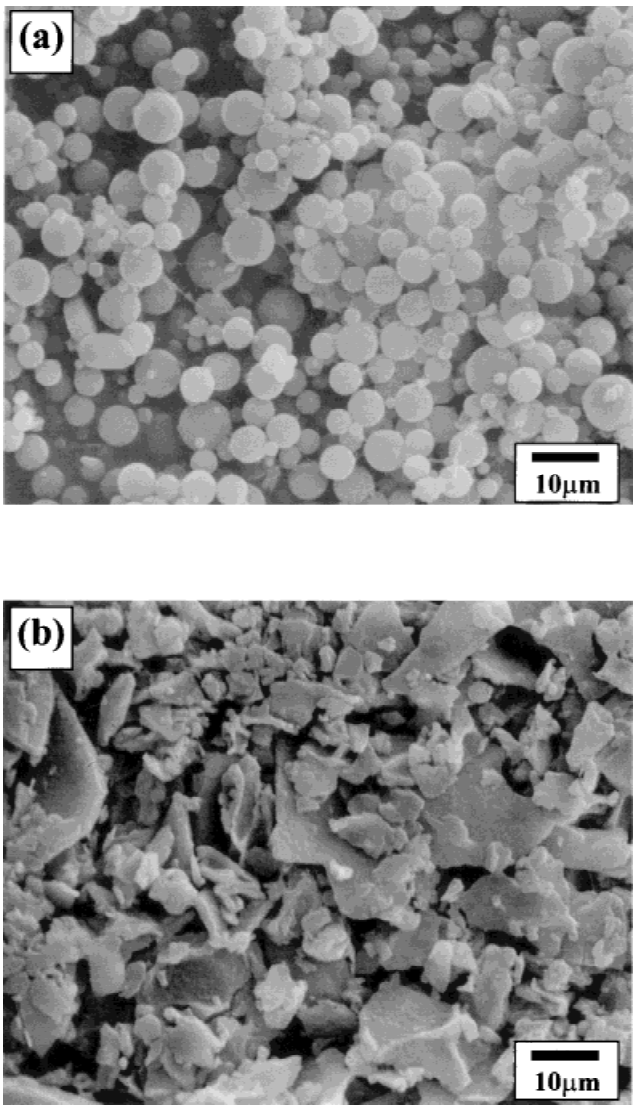


**Figure 2.** The SEM analysis of the morphology of (a) PLGA microspheres and (b) trypan blue powders. Scale bar = 10 μm.

PLGA in the methylene chloride and the mixing speed of the homogenizer during the emulsion process. The SEM analysis showed that the PLGA particles were spherical and had a smooth surface. Based on the image analysis of 50 particles, the size of the PLGA microspheres was found to be 1–7 μm in diameter with an average diameter of 4 μm. This value was consistent with 3.8 μm, which was the mean size of the PLGA microspheres from the laser scattering measurement. Figure 2(b) shows the morphology of the trypan blue particles from the freeze-drying procedure. The trypan blue particles are irregular in shape and mostly appear as flat flakes. The particles were less than 20-μm in length and width and approximately 2-μm in thickness. The PLGA microspheres and trypan blue powder were vigorously mixed by a vortex to allow the homogeneous distribution of the two components at the micron level in the solid state.

**Compression–heat molding**

The solid particle mixture of trypan blue powder and PLGA microspheres was fabricated into the shape of cylindrical millirods by a compression–heat molding procedure (Fig. 1). There are three essential parameters during fabrication that can affect the properties of the PLGA millirods: the fabrication temperature, annealing time, and compression pressure. The fabrication temperature was kept at a value higher than the $T_g$ of PLGA (45°C) to allow the annealing of the PLGA microspheres. During the annealing process a constant compression pressure was introduced to facilitate polymer annealing. The value of the compression pressure was $4.6 \times 10^6$ Pa (~46 times atmosphere pressure), as calculated by dividing the combined weight of the copper cylinder and aluminum cap over the cross-sectional area of the PLGA millirod. In this study the annealing time (2 h) and compression pressure were kept constant in all the experiments. The fabrication temperature was controlled at 60, 70, 80, and 90°C; the microstructures of the resulting PLGA millirods were characterized to correlate with their physical properties and release profiles.

**Microstructure of PLGA millirods by SEM analysis**

We used SEM to characterize the microstructures of the PLGA millirods to examine the extent of polymer annealing at different fabrication temperatures. Figure 3(a, b) shows the surface and cross section, respectively, of the PLGA millirod fabricated at 60°C. This fabrication temperature is 15°C higher than the $T_g$ of PLGA. At the millirod surface [Fig. 3(a)], polymer annealing occurred at the border of the microspheres as demonstrated by the merging boundaries. The extent of annealing, however, was far from complete because the PLGA microspheres and trypan blue particles maintained most of their original morphology. At the cross section of the millirod [Fig. 3(b)], the annealing was even less complete than that at the millirod surface, as indicated by the distinguished boundaries of the trypan blue powder and PLGA microspheres. These results demonstrated that the 60°C fabrication temperature produced poorly annealed millirods with rough surfaces and relatively loose internal structures. The observed microstructure was consistent with the lower density and flexual modulus of the 60°C millirods than those from higher fabrication temperatures (see results below).

PLGA millirods fabricated at 90°C showed completely different microstructures than the 60°C millirods. The SEM analysis for the surface and cross section of the 90°C millirods is presented in Figure 3(c, d),

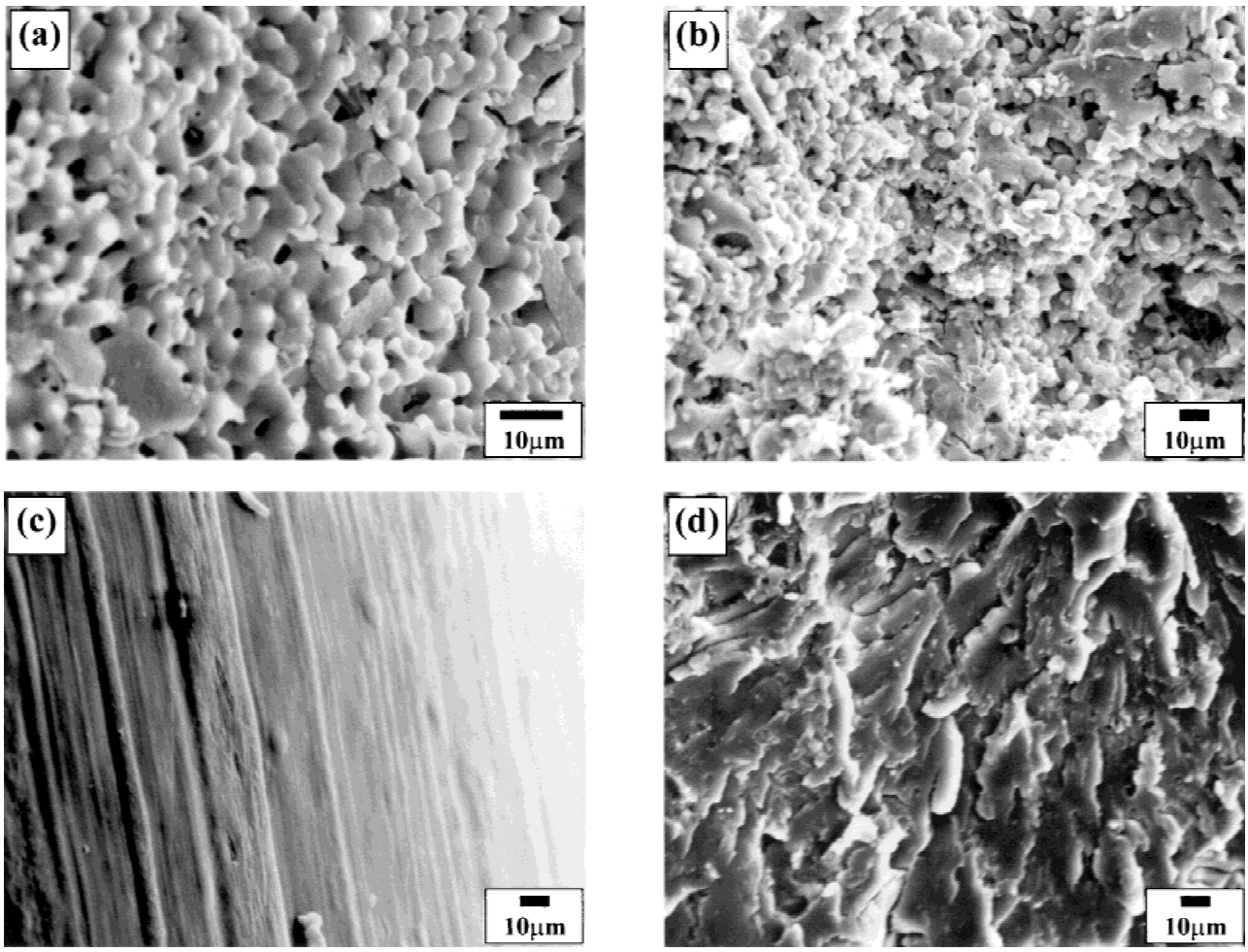


**Figure 3.** The SEM analysis of the microstructures of the PLGA millirods fabricated at 60 and 90°C: (a) the surface of the 60°C millirods, (b) the cross section of the 60°C millirods, (c) the surface of the 90°C millirods, and (d) the cross section of the 90°C millirods. Scale bars = 10 μm.

respectively. At the millirod surface, the original morphology of the PLGA microspheres and trypan blue powder disappeared completely. The surface appears to be smooth and the pattern of vertical lines reflects that of the internal surface of the Teflon tube used in fabrication. SEM analysis of the cross section of the millirod demonstrates uniform microstructures at different locations within the millirod [Fig. 3(d)]. PLGA microspheres appear to anneal completely with each other to form a condensed polymer phase. The trypan blue particles cannot be identified in the SEM image. Because the melting point of trypan blue (>300°C) is significantly higher than the fabrication temperature (90°C), the morphology of trypan blue powder is expected to be preserved after the fabrication process. The lack of observation of trypan blue powders may be a result of the complete polymer annealing and coverage surrounding the powders during compression–heat molding. The microstructure of the PLGA millirods fabricated at 80°C was similar to that at 90°C as described above.

The PLGA millirods fabricated at 70°C showed a different pattern of polymer annealing within the millirods [Fig. 4(a–d)]. Figure 4(a) illustrates the general overview of the cross section of the millirod under lower magnification. Gross inspection suggests two regions of different microstructures within the millirod. The region close to the millirod surface appears to be well annealed while the region close to the center of the millirod appears to be grainy. Figure 4(b–d) provides a detailed examination of the morphology at different locations on the millirod. At the millirod surface [Fig. 4(b)] the SEM analysis showed that the original shapes of the PLGA microspheres and trypan blue powders were mostly erased. Although some slight boundaries were still present, the overall surface morphology of 70°C millirods closely resembled that of the 90°C millirods. Within the millirod, the morphological appearance of the region close to the millirod surface was very similar to that of the 90°C millirods. The PLGA microspheres annealed completely to form a condensed polymer phase [Fig. 4(c)]. In com-

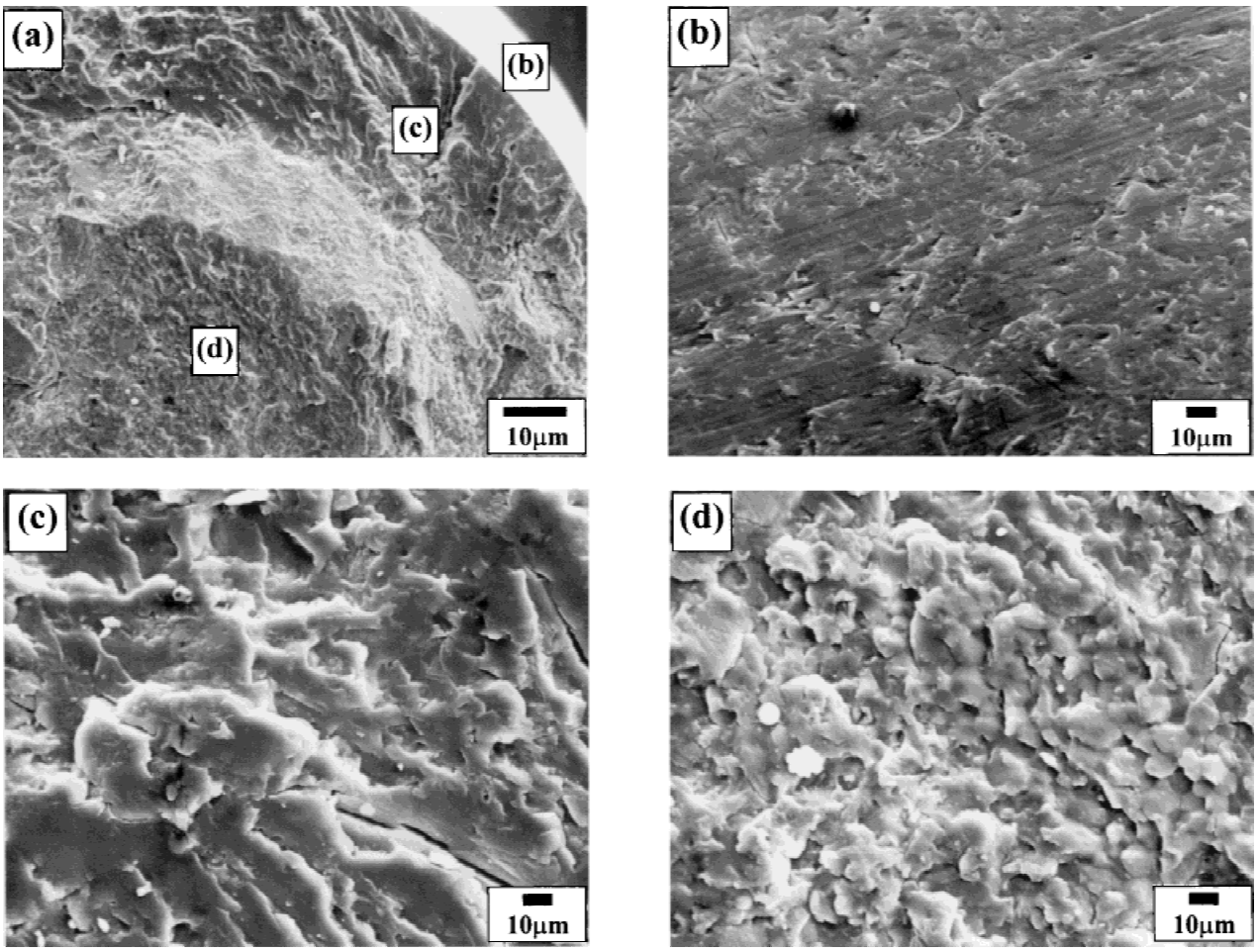


**Figure 4.** The SEM analysis of the microstructures of the PLGA millirods fabricated at 70°C: (a) the overview of the cross section of the PLGA millirod. Two distinguished layers (areas c and d) from the surface to the center of the millirod can be observed. Scale bar = 100 μm. (b) An SEM image of the surface of the millirod (area b in part a). Scale bar = 10 μm. (c) An image of the outer layer in the cross section of the PLGA millirod (area c in part a). The morphology is similar to that of the 90°C millirod [Fig. 3(d)]. Scale bar = 10 μm. (d) An image of the inner layer in the cross section of the millirod (area d in part a). Scale bar = 10 μm. The morphology is similar to that of the 60°C millirod [Fig. 3(b)].

parison, the region close to the center of the millirods [Fig. 4(d)] contained unannealed particles of PLGA microspheres and trypan blue powders. The particles had well-defined boundaries and led to relatively loose internal structures within the millirod.

This SEM study demonstrates that at a $4.6 \times 10^6$ Pa compression pressure and 2-h annealing time the 60 and 70°C temperatures are not sufficiently high for complete polymer annealing, although they are well above the $T_g$ of the PLGA polymer. The pattern of annealing in the 70°C millirods suggests a temperature gradient from the surface to the center of the millirod. Prolonging the annealing time or use of thinner Teflon tubes to reduce the barrier of heat transfer should lead to more completely annealed millirods. In the current procedure, we achieved the complete annealing of the PLGA polymer by raising the fabrication temperature to 80 or 90°C.

### Density and mechanical properties of millirods

We measured the density and flexural modulus of the PLGA millirods at different fabrication temperatures (Table I). The results showed that the density of the PLGA millirods increased with an increase in fabrication temperature from 60 to 90°C. The density value increased from 1.32 g/cm$^3$ for the 60°C millirods to 1.53 g/cm$^3$ for the 90°C millirods. The relative increase in density was approximately 16% for the 90°C millirods compared to the 60°C millirods. This value suggests that 90°C millirods will occupy 16% less volume compared to 60°C millirods of the same mass. This quantitative difference in density can be qualitatively correlated to the loose internal microstructures of the 60°C millirods as indicated by the SEM analysis.

The flexural modulus of the millirods produced at different fabrication temperatures was also measured

**TABLE I**
**Dependence of Density and Flexural Modulus of PLGA Millirods on Fabrication Temperature**

| Temperature (°C) | Density ($g/cm^3$)* | Modulus ($10^8$ Pa) | | |
|---|---|---|---|---|
| | | Average† | Maximum | Minimum |
| 60 | 1.32 ± 0.04 | 1.6 ± 0.5 | 2.3 | 0.6 |
| 70 | 1.36 ± 0.03 | 1.6 ± 0.4 | 2.0 | 0.9 |
| 80 | 1.47 ± 0.03 | 1.9 ± 0.1 | 2.2 | 1.8 |
| 90 | 1.53 ± 0.03 | 2.0 ± 0.1 | 2.2 | 1.7 |

*The average density and standard error are calculated from three samples.
†The average modulus and standard error are calculated from eight samples.

and compared. The average modulus was found to increase with an increase in the fabrication temperature. The average value of the modulus changed from $1.6 \times 10^8$ Pa for 60°C millirods to $2.0 \times 10^8$ Pa for 90°C millirods (Table I). Meanwhile, the standard deviation calculated from measurement of eight millirods at each fabrication temperature decreased from $0.5 \times 10^8$ Pa for 60°C millirods to $0.1 \times 10^8$ Pa for 90°C millirods. Table I also lists the maximum and minimum values of the flexural modulus within the group of millirods fabricated at the same temperature. The range of variation was significantly larger for millirods at lower fabrication temperatures than those at higher temperatures.

PLGA millirods fabricated at higher temperatures were mechanically stiffer and more reproducible, as shown by the flexural modulus, than those at lower fabrication temperatures. The higher modulus values for 80 and 90°C millirods were consistent with the complete polymer annealing in the millirods. In comparison, the relatively loose and slightly porous internal structures of the 60°C millirods should lead to weaker and more unpredictable mechanical properties. Variations in mechanical properties may suggest that the millirods have different microstructures or extent of polymer annealing, which can lead to erratic or unpredictable release profiles for millirods from identical fabrication conditions. For a majority of these millirods, their flexural moduli were above $1 \times 10^8$ Pa (comparable to medium density polyethylene), which is sufficiently strong for direct implantation in tumor tissues for local drug therapy.

### Distribution of trypan blue within PLGA millirods

The distribution of trypan blue in the PLGA millirods is an important factor that affects the reproducibility of the release profile of the dye. Here we developed a $\Delta c_p$ method to determine the loading density of trypan blue at different sections of the PLGA millirod by DSC. DSC experiments allow the measurement of the specific heat capacity ($c_p$) as a function of temperature for a given temperature range. The $c_p$ is defined as the amount of heat ($\partial H$) required to raise the temperature ($\partial T$) at a constant pressure ($p$) per unit mass of a material [Equation (1)]. For a material containing two components without interactions, the $c_p$ of the binary mixture is equal to the sum of the products of the mass percentage for each component and the $c_p$ for the pure component. Equation (2) describes this relationship in the PLGA millirods,

$$c_p = \frac{1}{m}\left(\frac{\partial H}{\partial T}\right)_p \tag{1}$$

$$c_p\,(\text{millirod}) = \frac{m_{\text{PLGA}}}{M}\,c_p\,(\text{PLGA}) + \frac{m_{\text{TB}}}{M}\,c_p(\text{TB}) \tag{2}$$

where $c_p$(millirod), $c_p$(PLGA), and $c_p$(TB) are the $c_p$ values for the PLGA millirod containing trypan blue, the PLGA polymer, and pure trypan blue, respectively. The terms $m_{\text{PLGA}}$, $m_{\text{TB}}$, and $M$ represent the mass of the PLGA polymer, trypan blue, and PLGA millirod, respectively. The value of $m_{\text{TB}}/M$ is also defined as the loading density of trypan blue in the PLGA millirod.

In the $\Delta c_p$ method, we measured the change in the $c_p$ before and after the glass transition of the PLGA polymer. Because the current PLGA polymer with a 1:1 glycolide:lactide ratio is completely amorphous, the $\Delta c_p$ value reflects the $c_p$ changes between the rubbery and glassy states for the total mass of the polymer. The DSC experiments were carried out in the temperature range between 10 and 80°C. Within this temperature range the experimental results showed that the value of $\Delta c_p$ for trypan blue was approximately zero. Based on this result and Equation (2), we obtained Equation (3),

$$\Delta c_p(\text{millirod}) = \frac{m_{\text{PLGA}}}{M}\,\Delta c_p(\text{PLGA}) \tag{3}$$

$$LD = \frac{m_{\text{TB}}}{M} = 1 - \frac{m_{\text{PLGA}}}{M} = 1 - \frac{\Delta c_p(\text{millirod})}{\Delta c_p(\text{PLGA})} \tag{4}$$

where the value of $\Delta c_p$(millirod) is equal to the product of the mass percentage of the PLGA polymer and the value of $\Delta c_p$(PLGA). Equation (4) describes the principle of the $\Delta c_p$ method in the measurement of the loading density (LD) of trypan blue in the PLGA millirods.

Figure 5(a) shows the DSC curves for the pure PLGA polymer and a representative section of the PLGA millirod. The DSC curve is plotted in the $c_p$ as a function of temperature. The $T_g$ and $\Delta c_p$ can both be measured from the DSC curve. The $T_g$ value was determined by extending the tangents of the curve immediately proceeding and following the glass transition, then measuring the temperature at one-half the vertical distance between the two lines. The $\Delta c_p$ value was determined as the whole vertical distance. The $T_g$ values for pure PLGA polymer and tryphan blue-containing PLGA millirods were both 44.6 ± 0.1°C.

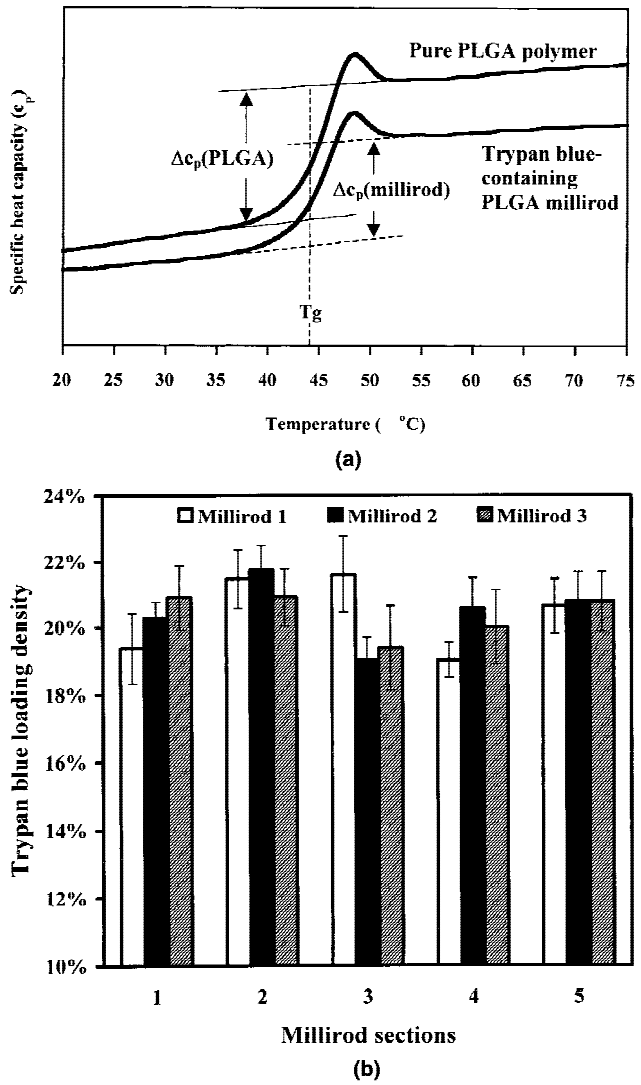


**Figure 5.** (a) Representative DSC thermograms of pure PLGA polymer and a small section of the PLGA millirod containing trypan blue. The $T_g$ values for the pure PLGA polymer and PLGA millirod were determined to both be 44.6 ± 0.1°C. The values of the $\Delta c_p$ for the pure PLGA polymer and PLGA millirod were 0.474 and 0.384 J/(g °C), respectively. (b) The measurement of the loading density of trypan blue at different sections of three PLGA millirods by the $\Delta c_p$ method. The loading densities were determined according to Equation (4). The error bars show the standard deviation of the loading density in three $\Delta c_p$ measurements.

The identical $T_g$ values indicated that the PLGA polymer in the millirod containing trypan blue had the same thermal properties as the pure PLGA polymer. We determined the loading densities of trypan blue in different sections of the PLGA millirods based on the $\Delta c_p$ values using Equation (4). Figure 5(b) illustrates the values of the loading density for five different sections of the three PLGA millirods. The experimental results showed that the loading density of trypan blue in all the sections of different PLGA millirods was 20 ± 2% by the $\Delta c_p$ method. This result was consistent with the value calculated from the weight measurement before the fabrication. Furthermore, the loading density of each section of the three millirods was within experimental uncertainty (±2%), which demonstrated a homogeneous distribution of trypan blue within the same millirod and between different millirods. Therefore, the PLGA millirods have satisfactory composition homogeneity for controlled release applications.

The $\Delta c_p$ method should make a useful addition to the existing methodology for the measurement of drug loading densities in drug delivery devices. Currently, the most common method to measure the drug loading density is the solvent extraction procedure in which the drug is extracted into either an organic or aqueous phase (depending on the solubility and polarity of the drug) for quantitative measurement. Sometimes the procedure is complicated by the partition of the agent in both phases, or difficulty in achieving a clean phase separation for spectrophotometric measurement, or drug decomposition by organic solvents or the use of a strong base in the aqueous phase. In the tryphan blue-containing PLGA millirods we experienced the first two complications, which prevented the satisfactory quantification of the dye loading densities. The $\Delta c_p$ method avoided such complications and provided an alternative method to determine this parameter. However, it should be noted that the $\Delta c_p$ method also has its own limitations. For example, this method is only applicable to polymer-based systems that have glass transition phenomena. The sensitivity of the measurement depends on the magnitude of change in the heat capacity of the polymer and the sensitivity of the DSC instrument (the experimental uncertainty for PLGA systems in this study was 2%). Furthermore, the $\Delta c_p$ method is not directly applicable for polymers that contain a crystalline phase. In this case, quench cooling may be necessary to eliminate the crystalline phase for the measurement of the $\Delta c_p$ that corresponds to the total mass of the polymer. Despite these limitations, the $\Delta c_p$ method provides a new and alternative procedure for the measurement of drug loading density in polymer-based systems.

## Release properties of PLGA millirods

Figure 6 compares the release profiles of PLGA millirods fabricated at different temperatures. For each fabrication temperature, the release profiles of three millirods were measured and compared to evaluate the reproducibility in the release properties. Each release profile is represented by the percentage of released trypan blue as a function of the release time. The results from Figure 6(a) show that the release rate

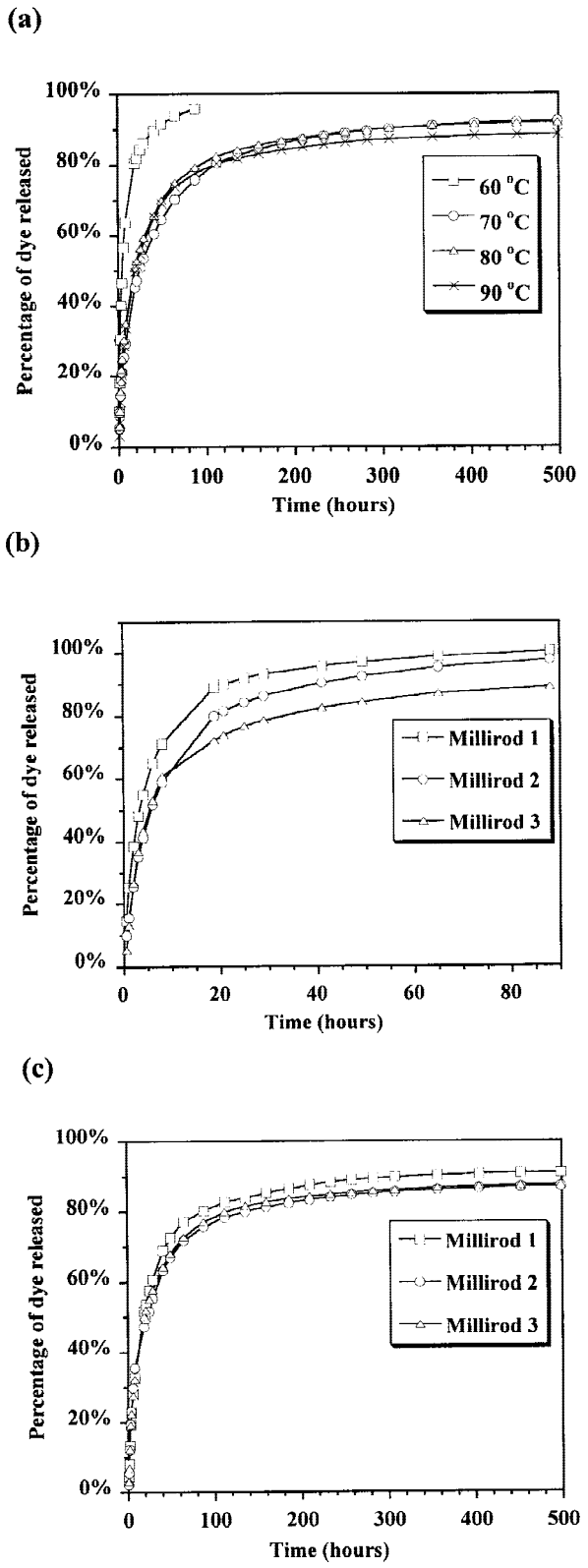


**Figure 6.** Release profiles of trypan blue-containing PLGA millirods that were fabricated at different temperatures. (a) The average release curves of millirods fabricated at 60, 70, 80, and 90°C. For clarity of presentation, the error bars in the release percentage for each time point are not shown. The standard error varies between 5 and 15, 3 and 10, 2 and 9, and <4% for 60, 70, 80, and 90°C millirods, respectively. (b) The release curves of three millirods fabricated at 60°C. (c) The release curves of three millirods fabricated at 90°C. The release studies were carried out in PBS at 37°C.

of trypan blue from 60°C millirods is faster than those at higher fabrication temperatures. After 50 h approximately 90% of the dye in the 60°C millirod was released, but for the 90°C millirods it took more than 500 h to release 90% of the dye. We also determined the values of the time for 50% of the trypan blue to be released ($t$½) for millirods at different fabrication temperatures. The average $t$½ values for 60, 70, 80, and 90°C millirods were 5, 25, 25, and 25 h, respectively. The faster release rates for 60°C millirods were consistent with the loose and relatively porous microstructures within the PLGA millirods. The existence of the pores and possible channels may facilitate the diffusion of water into the PLGA millirods, as well as the release of trypan blue from the millirod into solution. The release kinetics of the 70°C millirods was more similar to that of the 80 and 90°C millirods than to the 60°C millirods. Although the SEM analysis showed that the regions close to the center of the 70°C millirods were also grainy and unannealed, we hypothesize that their release kinetics were primarily dictated by the well-annealed exterior section, which is similar to the 80 and 90°C millirods.

We also evaluated the reproducibility of the release profiles for different PLGA millirods fabricated at the same temperature. Figure 6(b, c) shows the release profiles for three millirods fabricated at 60 and 90°C, respectively. The variation in the release rates between the 60°C millirods is significant [Fig. 6(b)]. For example, at the 20-h point, the maximum difference in the percentage of released trypan blue between two millirods is almost 20%. This variation is not acceptable in controlled release applications, especially for anticancer drugs with a narrow therapeutic index. In contrast, the maximum difference in the release percentage is less than 5% at any time points for the 90°C millirods. We also calculated the standard deviation in the release percentage at different time points based on the release profiles of three millirods at each fabrication temperature. For the 60°C millirods, the standard deviation varies from 5–15%; for millirods fabricated at 70 and 80°C, the standard deviation varies in the ranges of 3–10 and 2–9%, respectively. The 90°C millirods showed the most reproducible release profiles among the three individual millirods [Fig. 6(c)]. Throughout the release studies, the standard deviation in the percentage of release at any time point was less than 4%. The superb reproducibility in the release kinetics for the 90°C millirods demonstrated the optimal fabrication conditions for PLGA millirods.

## CONCLUSIONS

This article described a compression–heat molding procedure for the fabrication of PLGA millirods for local cancer therapy. SEM analysis was used to exam-

ine the microstructures of the PLGA millirods from different fabrication temperatures. The results showed that the millirods fabricated at 60°C maintained the original morphology of most of the PLGA microspheres and trypan blue powder. In comparison, millirods fabricated at 80 and 90°C showed well-annealed and dense internal microstructures. The density, flexural modulus, composition homogeneity, and release profiles of the PLGA millirods were also characterized and compared. The values of the density and flexural modulus increased with an increase in the fabrication temperature. The release studies showed that 90°C millirods have the most reproducible release profiles. The results from this study demonstrated that the optimal fabrication conditions for PLGA millirods were 90°C fabrication temperature for 2 h at a compression pressure of $4.6 \times 10^6$ Pa. The resulting PLGA millirods had sufficient mechanical strength, homogeneous agent distribution, and reproducible release profiles for controlled release applications. Work is currently in progress to fabricate PLGA millirods that contain anticancer drugs (e.g., doxorubicin, carboplatin) for the local treatment of liver tumors.

We thank Dr. John Haaga, Dr. Nicholas Stowe, and Dr. Sergei Nazaranko for helpful discussions.

## References


1. Gillams AR, Lees WR. Survival after percutaneous, image-guided, thermal ablation of hepatic metastases from colorectal cancer. Dis Colon Rectum 2000;43:656–661.
2. Boppart SA, Herrmann J, Pitris CL, Stamper DL, Brezinski ME, Fujimoto JG. High-resolution optical coherence tomography-guided laser ablation of surgical tissue. J Surg Res 1999;82:275–284.
3. Morocz IA, Hynynen K, Gudbjartsson H, Peled S, Colucci V, Jolesz FA. Brain edema development after MRI-guided focused ultrasound treatment. J Magn Reson Imaging 1998;8: 136–142.
4. Devaux BC, Roux FX. Experimental and clinical standards, and evolution of lasers in neurosurgery. Acta Neurochir 1996;138: 1135–1147.
5. Campbell DC. Thermoablation treatment for trichiasis using the argon laser. Aust NZ J Ophthalmol 1990;18:427–430.
6. Steiner P, Botnar R, Dubno B, Zimmermann GG, Gazelle GS, Debatin JF. Radiofrequency-induced thermoablation: Monitoring with T1-weighted and proton-frequency-shift MR imaging in an interventional 0.5-T environment. Radiology 1998;206: 803–810.
7. Allgaier HP, Deibert P, Zuber I, Blum HE. Percutaneous treatment of liver tumors using interstitial radiofrequency thermoablation. A new therapeutic strategy. Dtsch Med Wochenschr 1998;123:907–911.
8. Marone G, Francica G, D'Angelo V, Iodice G, Pastore P, Altamura G, Cusati B, Siani A. Echo-guided radiofrequency percutaneous ablation of hepatocellular carcinoma in cirrhosis using a cooled needle. Radiol Med (Torino) 1998;95:624–629.
9. Sack MJ, Weber RS, Weinstein GS, Chalian AA, Nisenbaum HL, Yousem DM. Image-guided fine-needle aspiration of the head and neck: Five years' experience. Arch Otolaryngol Head Neck Surg 1998;124:1155–1161.
10. Maroon JC, Onik G, Quigley MR, Bailes JE, Wilberger JE, Kennerdell JS. Cryosurgery re-visited for the removal and destruction of brain, spinal and orbital tumours. Neurol Res 1992;14: 294–302.
11. Germer CT, Albrecht D, Roggan A, Buhr HR. Technology for *in situ* ablation by laparoscopic and image-guided interstitial laser hyperthermia. Semin Laparosc Surg 1998;5:195–203.
12. Hahn PF, Gazelle GS, Jiang DY, Compton CC, Goldberg SN, Mueller PR. Liver tumor ablation: Real-time monitoring with dynamic CT. Acad Radiol 1997;4:634–638.
13. Layer G. Image-guided interventions in liver tumors. Radiologe 1999;39:750–755.
14. Merkle EM, Boll DT, Boaz T, Duerk JL, Chung YC, Jacobs GH, Varnes ME, Lewin JS. MRI-guided radiofrequency thermal ablation of implanted VX2 liver tumors in a rabbit model: Demonstration of feasibility at 0.2 T. Magn Reson Med 1999;42:141–149.
15. Miao Y, Ni Y, Mulier S, Yu J, De Wever I, Penninckx F, Baert AL, Marchal G. Treatment of VX2 liver tumor in rabbits with "wet" electrode mediated radio-frequency ablation. Eur Radiol 2000;10:188–194.
16. Greenlee RT, Murray T, Bolden S, Wingo PA. Cancer statistics, 2000. CA Cancer J Clin 2000;50:7–33.
17. Goldberg SN, Mallery S, Gazelle GS, Brugge WR. EUS-guided radiofrequency ablation in the pancreas: Results in a porcine model. Gastrointest Endosc 1999;50:392–401.
18. Merkle EM, Haaga JR, Duerk JL, Jacobs GH, Brambs HJ, Lewin JS. MR imaging-guided radio-frequency thermal ablation in the pancreas in a porcine model with a modified clinical C-arm system. Radiology 1999;213:461–467.
19. McGovern FJ, Wood BJ, Goldberg SN, Mueller PR. Radio frequency ablation of renal cell carcinoma via image guided needle electrodes. J Urol 1999;161:599–600.
20. Zlotta AR, Windschutz T, Raviv G, Peny MO, van Gansbeke D, Noel JC, Schulman CC. Radiofrequency interstitial tumor ablation (RITA) is a possible new modality for treatment of renal cancer: *Ex vivo* and *in vivo* experience. J Endourol 1997;11:251–258.
21. Lewin JS, Connell CF, Duerk JL, Chung YC, Clampitt ME, Spisak J, Gazelle GS, Haaga JR. Interactive MRI-guided radiofrequency interstitial thermal ablation of abdominal tumors: Clinical trial for evaluation of safety and feasibility. J Magn Reson Imaging 1998;8:40–47.
22. Hall-Craggs MA. Interventional MRI of the breast: Minimally invasive therapy. Eur Radiol 2000;10:59–62.
23. Jeffrey SS, Birdwell RL, Ikeda DM, Daniel BL, Nowels KW, Dirbas FM, Griffey SM. Radiofrequency ablation of breast cancer: First report of an emerging technology. Arch Surg 1999; 134:1064–1068.
24. Dodd GD 3rd, Soulen MC, Kane RA, Livraghi T, Lees WR, Yamashita Y, Gillams AR, Karahan OI, Rhim H. Minimally invasive treatment of malignant hepatic tumors: At the threshold of a major breakthrough. Radiographics 2000;20:9–27.
25. Lencioni R, Goletti O, Armillotta N, Paolicchi A, Moretti M, Cioni D, Donati F, Cicorelli A, Ricci S, Carrai M, et al. Radiofrequency thermal ablation of liver metastases with a cooled-tip electrode needle: Results of a pilot clinical trial. Eur Radiol 1998;8:1205–1211.
26. Francica G, Marone G. Ultrasound-guided percutaneous treatment of hepatocellular carcinoma by radiofrequency hyperthermia with a "cooled-tip needle." A preliminary clinical experience. Eur J Ultrasound 1999;9:145–153.
27. Buscarini L, Rossi S. Technology for radiofrequency thermal ablation of liver tumors. Semin Laparosc Surg 1997;4:96–101.

28. Murakami H, Kobayashi M, Takeuchi H, Kawashima Y. Utilization of poly(DL-lactide-*co*-glycolide) nanoparticles for preparation of mini-depot tables by direct compression. J Controlled Release 2000;67:29–36.
39. Chowdhury DK, Mitra AK. Kinetics of a model nucleotide (guanosine) release from biodegradable poly(DL-lactide-*co*-glycolide) microspheres: A delivery system for long-term intraocular delivery. Pharm Dev Technol 2000;5:279–285.
30. Emerich DF, Tracy MA, Ward KL, Figueiredo M, Qian R, Henschel C, Bartus RT. Biocompatibility of poly (DL-lactide-*co*-glycolide) microspheres implanted into the brain. Cell Transplant 1999;8:47–58.
31. Ertl B, Platzer P, Wirth M, Gabor F. Poly(D,L-lactic-*co*-glycolic acid) microspheres for sustained delivery and stabilization of camptothecin. J Controlled Release 1999;61:305–317.
32. Mandal TK. Development of biodegradable drug delivery system to treat addiction. Drug Dev Ind Pharm 1999;25:773–779.
33. Fishbein I, Chorny M, Rabinovich L, Banai S, Gati I, Golomb G. Nanoparticulate delivery system of a tyrphostin for the treatment of restenosis. J Controlled Release 2000;65:221–229.
34. Radwan MA, Zaghloul IY, Aly ZH. *In vivo* performance of parenteral theophylline-loaded polyisobutylcyanoacrylate nanoparticles in rats. Eur J Pharm Sci 1999;8:95–98.
35. Losa C, Calvo P, Castro E, Vila–Jato JL, Alanso MJ. Improvement of ocular penetration of amikacin sulphate by association to poly(butylcyanoacrylate) nanoparticles. J Pharm Pharmacol 1991;43:548–552.
36. Labhasetwar V, Song C, Humphrey W, Shebuski R, Levy RJ. Arterial uptake of biodegradable nanoparticles: Effect of surface modifications. J Pharm Sci 1998;87:1229–1234.